International Journal of Modern Agriculture, Volume 10, No.2, 2021
ISSN: 2305-7246

Design And Fabrication Of Al-Si (Er4043) Aluminium Impeller Using Wire Arc Additive Manufactured (Waam)

Manikandan.N[1*], Dr. G. Swaminathan [2], Yedula Ajith Reddy[3], Akhil Varier P V[4], D Hari Hara[5], Bharath Chandra[6], E Vijayaragavan[7]

[1] Research Scholar, SRM Institute of Science and Technology, Ramapuram, Tamil Nadu, India
[3,4,5] UG - Students, SRM Institute of Science and Technology, Ramapuram, Tamil Nadu, India
[2, 6] Assistant Professor, Department of Mechanical Engineering, SRM Institute of Science and Technology, Tamil Nadu. India
Email: [1]manisrm2011@gmail.com, [7]vijayare@srmist.edu.in

Abstract

Wire arc additive manufacturing (WAAM) is amassing the curiosity of many researchers as well as industry specialists, because of its high deposition rates, low buy-to-fly ratio (BTF), low investment, and good material properties of manufactured products. WAAM produces components layer by layer using MIG/TIG welding. When compared with other additive manufacturing techniques such as Direct Metal Laser Sintering (DMLS) which uses raw material in the form of powder which is quite difficult to produce and has a high price tag, WAAM uses wire which have advantages in both price and is easy to produce. WAAM is very beneficial for manufacturing large/big components with medium complexity. This paper presents the final results obtained from mechanical testing conducted on an impeller prototype fabricated using WAAM along with the design and analysis of the impeller. And a detailed explanation of the whole process of fabricating the impeller prototype using WAAM is provided.

Key words: WAAM, Additive Manufacturing, Welding, Microstructure, Chemical Composition, Brinell Hardness Test

Introduction

Impeller is an essential rotating part in centrifugal pumps, which are involved in our daily life inseparably. Pumps are classified into radial, axial, and mixed flow pumps. Type of impeller used in the pump decide the category of the pump. The propeller, turbine also falls under the category of the impeller.

Nowadays the majority of the impellers are manufactured using either CNC machining or foundry (Casting). Both have major disadvantages such as Casting takes up a lot of space and the complexity of the impeller has to be low and in CNC machining, a lot of material is wasted as scrap. Additive manufacturing (AM) can be used to overcome material wastage, adding to the advantage that it takes less space. In additive manufacturing, parts are manufactured by depositing material layer by layer. There are different types of additive manufacturing processes currently under research. Even though the core idea is the same in all the processes i.e., creating part layer by layer, there are differences in how each layer is created in different processes. Some of the renowned additive manufacturing techniques are Powder bed fusion (PBF), Wire Arc Additive Manufacturing (WAAM) and Sheet Lamination. Powder bed fusion creates component by spreading a thin layer of powder on top, then the powder is fused with the help of a laser. This process is repeated until the completion of the component. Powder bed fusion is further divided into different categories, Direct Metal Laser Sintering (DMLS) in which each layer is sintered not melted, Selective Laser Melting (SLM) in which each layer is fused by melting the powder. Wire Arc Additive Manufacturing creates components by directly depositing the metal on top of each layer. WAAM uses different welding techniques for the deposition of metal, such as Gas Metal Arc Welding (GMAW), Cold Metal Transfer (CMT), Plasma Arc Welding (PAW), and Gas Tungsten Arc Welding (GTAW). Each has its advantages and disadvantages. For this project, we used Gas Metal Arc Welding (GMAW).

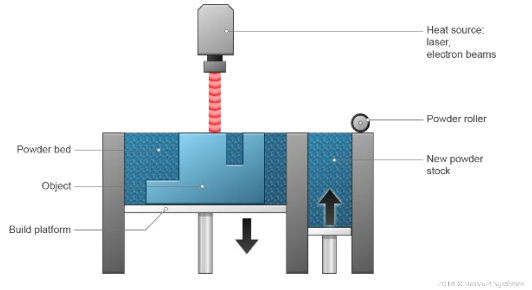

Fig 1.1 Powder Bed Fusion

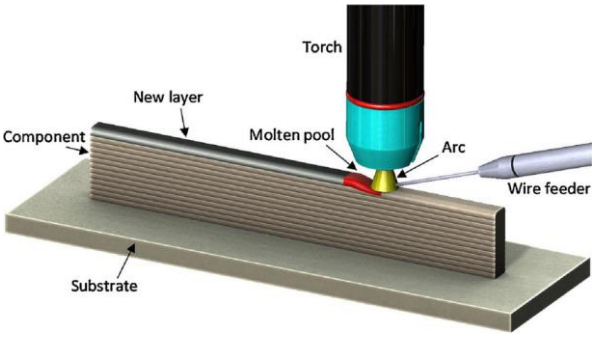

Fig 1.2 Wire Arc Additive Manufacturing

Materials and Methods

An aluminium wire of thickness 1.2mm is used for 3d printing the impeller. Al 5356 and AL 4043 are used as feedstock material. An aluminium (Grade 6061) sheets with 8mm and 16mm thickness is used as a base plate.

The robotic arm used for the printing is Yaskawa Motoman GP12 (Fig 2.1), which has a horizontal reach of 1440mm and vertical reach of 2511mm. Robot's payload is 12Kg and has repeatability up to 0.02mm. GP12 uses the YRC 1000 controller (Fig 2.2) for the code input, code compilation, and for sending inputs for the robot.

Welding Equipment used are Kemppi A7 power source 450 (Fig 2.3) and A7 MIG welder. The wire feeder used is A7 Wire Feeder 25 (Fig 2.4), which operates on a 4-roll, two motors mechanism. Wire feeder has a feed speed range of 0.5m to 25m/min. Operating wire sizes for Aluminium are 1mm to 2.4mm.

2.1 Yaskawa Motoman GP12

2.2 Yaskawa YRC1000 Controller

Aluminium wire is deposited onto the base plate using Metal Inert Gas Welding (MIG) also popularly known as arc welding. In this method, electrons jump from the electrode (connected to the negative terminal) to the workpiece (connected to the positive terminal) generating heat required to melt the feedstock material. Shielding

gas used to reduce oxidation and increase penetration. Shielding gas used consists of Argon (Ar) and Helium (He). Argon helps in reducing oxidation and Helium increases penetration.

2.3 Kemppi A7 Power Source 450

2.4 Kemppi A7 wire Feeder 25

2.1 Design

For the design of the impeller, SolidWorks software is used. SolidWorks is a cad cam software. Impeller dimensions are calculated using pre-defined pump parameters such as Head (H), Speed (N) and working fluid flow rate (Q). Using these pre-defined parameters, dimensions such as specific speed, Efficiency, Inlet Diameter, Outlet Diameter, Inlet Blade angle, and Outlet Blade angle are calculated.

Pre-defined Pump parameters

Head (H) = 14 m

Flow rate (Q) = $16 * 10^{-3}$ m^3/s = 16 Kg/s

Speed (N) = 1800 rpm = 188.5 rad/s

Working fluid Density = 1000 kg/m^3

Specific Speed:

$$N_s = \frac{3.65 n \sqrt{Q}}{(H)^{3/4}}$$

$$N_s = \frac{3.65 * 1800 * \sqrt{0.016}}{(14)^{3/4}}$$

$$N_s = 115.2$$

Inlet Diameter:

$$D_1 = 4.5 * 10^3 * \sqrt[3]{(Q/n)}$$

$$D_1 = 4.5 * 10^3 * \sqrt[3]{(0.016/1800)}$$

$$D_1 = 90mm$$

Efficiency:

$\eta_h = 1 - 0.42/(\log(D_1) - 0.172)^2 = 0.87 = 87\%$

$\eta_v = 1/(1 + 0.68 * N_s^{-2/3}) = 0.968 = 96.8\%$

$\eta_m = 0.96 = 96\%$

$\eta = \eta_h * \eta_v * \eta_m = 0.81 = 81\%$

Inlet Angle:

$Q_{th} = Q/ \eta_v = 0.0165\ m^3/s$

$C_{m0} = 0.06 * \sqrt[3]{(Q_{th} * n^2)} = 2.26\ m/s$

$C_{m1} = K_1 * C_{m0} = 1.4 * 2.26 = 3.16\ m/s$

$U_1 = \pi * D_1 * n/60$

$U_1 = \pi * 0.09 * 1800/60 = 8.5\ m/s$

$\beta_{10} = Arctan(C_{m1}/U_1) = 20.5^o$

$\beta_1 = \beta_{10} + \delta = 20.5 + 4.5 = 25^o$

Using the above dimensions, a 3d cad model is designed in SolidWorks software. The model is scaled down by 50% to reduce the printing time and material consumption. The resulting model has an outer diameter of 100mm and a height of 20mm. With these geometric dimensions, printing takes about 50 minutes.

Outlet Diameter:

$H_m = H/ \eta_h = 17.23\ m$

$U_2 = \sqrt{(g * H_m / C_{u2})} = 18.45\ m/s$

$D_2 = 60 * U_2 / \pi * n = 196\ mm$

Outlet Angle:

$C_{m3}/C_{m0} = 0.8$

$w_1/w_2 = 1.18$

$K_1 = 1.4$

$K_2 = 1.2$

$Sin\ \beta_2 = Sin\ \beta_1 * (K_2/K_1) * (w_1/w_2) * (C_{m3}/C_{m0}) = 0.987$

U – Blade velocity

C – Absolute velocity

W – Relative Velocity

α – Absolute Angle

β – Blade Angle

Suffix 0,1,2,3 indicates conditions before entrance, at entrance, at outlet, after outlet respectively.

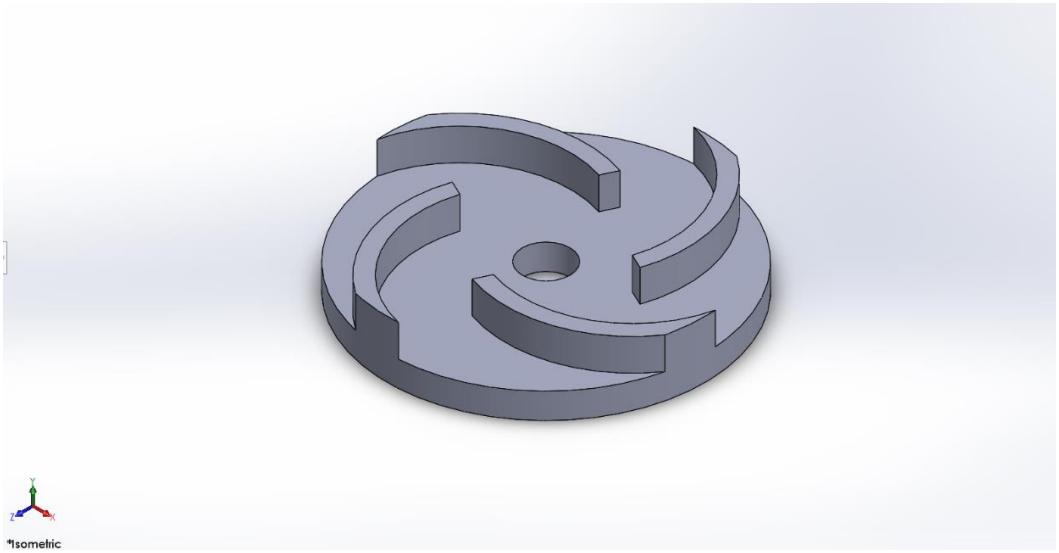

2.5 Design of Impeller in SolidWorks

2.2 Analysis

Structural analysis of the impeller is done using Ansys Software. Using the Ansys software Deformation, stress, and strain acting on the impeller, due to rotating at high speeds, are calculated.

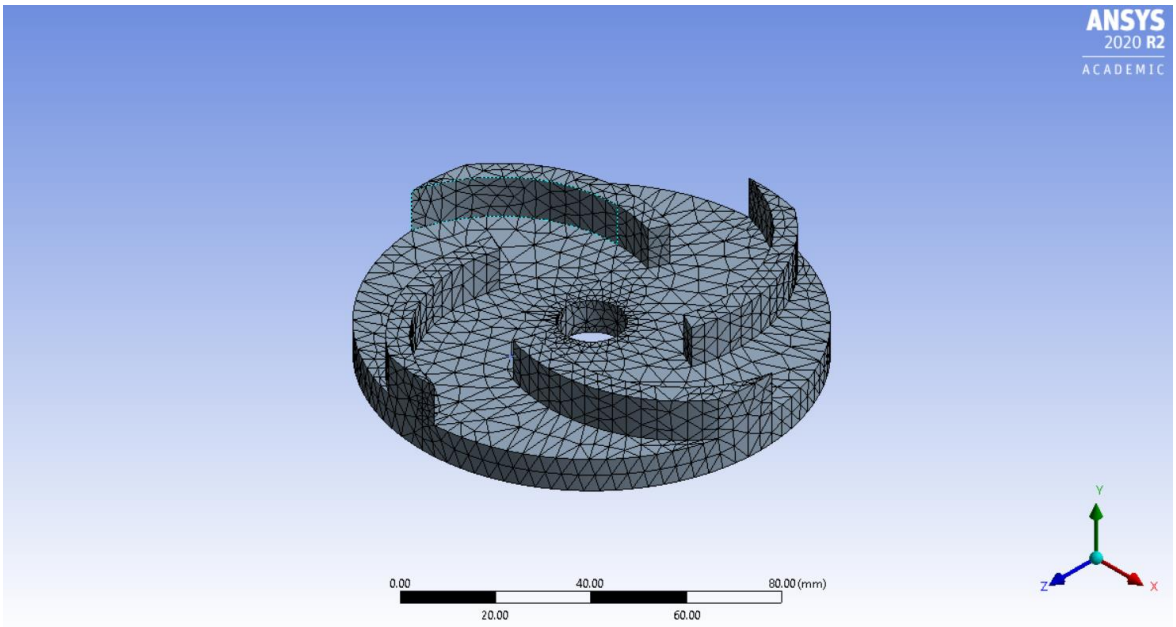

2.6 Mesh Model of the Impeller

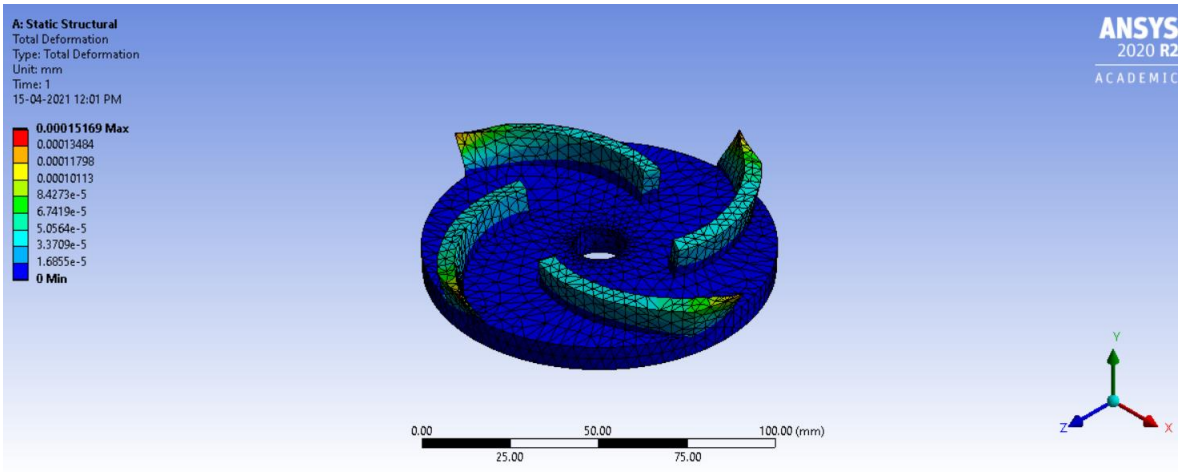

2.7 Total Deformation

For Meshing the impeller cad model refinement is used to obtain fine meshing. Deformation (Fig 2.7) of the impeller due to rotating at 1800 rpm is found out to be 0.00015mm and Maximum stress is 0.18MPa with average stress (Fig 2.8) of 0.03MPa. Maximum strain acting on the impeller is 2.96 * 10^{-6} while the average strain (Fig 2.9) is 6.33 * 10^{-7}

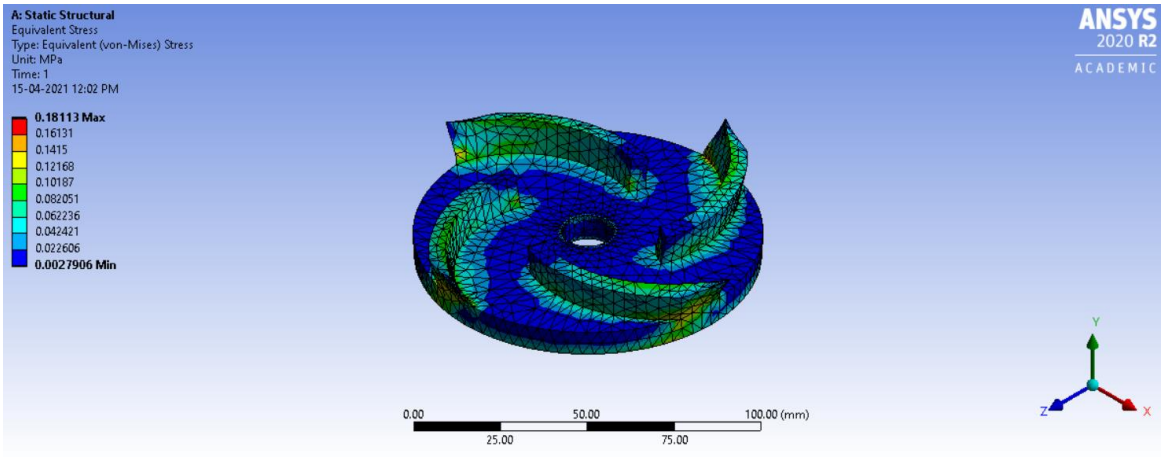

2.8 Stress

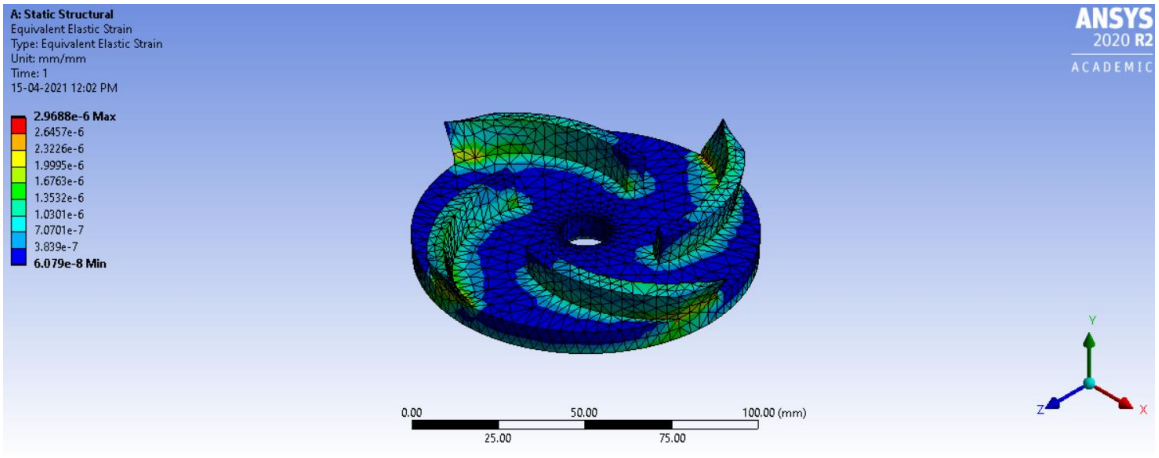

2.9 Strain

2.3 Fabrication

Fabrication of the impeller is done with the help of the Robotic arm Yaskawa Motoman GP12. Metal Inert Gas Welding equipment is attached to the robotic arm. Welding equipment used are Kemppi A7 MIG Weld torch and Kemppi A7 Power Source 450. Kemppi wire feeder 25 is used to feed the wire into the weld gun. Wire feeder has an operating range of 1mm to 2.4mm wire diameter for aluminium. To control the robotic arm Yaskawa YRC1000 is used.

Welding Parameters are set in the power source, such as current, and voltage. Now G-Code is prepared for the robotic arm. G-Code is a universally accepted format for CNC machines, Robotic arms, 3d Printers and many more. G-Code contains the path that has to be followed, feed rate, velocity and thickness of each layer.

For the fabrication Aluminium 4043 and Aluminium 5356 are used in the form of wire as feedstock material. The wire diameter is 1.2mm which is within the operating range of the wire feeder. Aluminium 6061 is used as a baseplate with varied thickness one 8mm thick and the other with 16mm thickness.

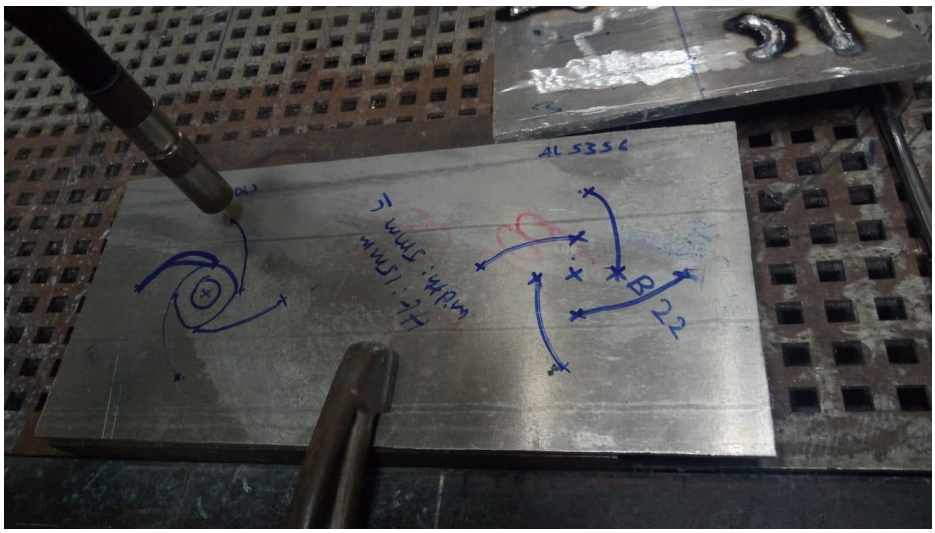

2.10 Pre-Welding

2.11 First Layer

2.12 Fully Printed Part

Welding Parameters

Welding parameters such as voltage and current are different for the first two layers than the rest of the layers. This is because higher current and voltage increases the fusion of weld material with the base material. For the first two layers on an 8mm thick base plate Wire feed speed, current, and voltage are 6m.min, 160A, and 22.5V respectively. The remaining parameters are the same for every layer.

Table 2.1 Welding Parameters from 3rd layer onward

Wire Feed Speed	7 m/min
Travel Speed	40 cm/min
Shielding Gas	100% Argon (Ar)
Gas Flow Rate	15 LPM
Angle	90^{o}
Current	160 A
Voltage	21.5 V

Table 2.1 shows all the welding parameters for each layer from the 3rd layer onwards for the impeller. Current, voltage and wire feed rate change for the first 2 layers depending on the materials used and thickness of the base plate used. As base plate thickness increases voltage, current, and wire feed speed should also increase. For the first 3 layers on 16mm thick base plate wire feed speed, voltage, and current are 9 m/min, 26 V, and 170 A respectively.

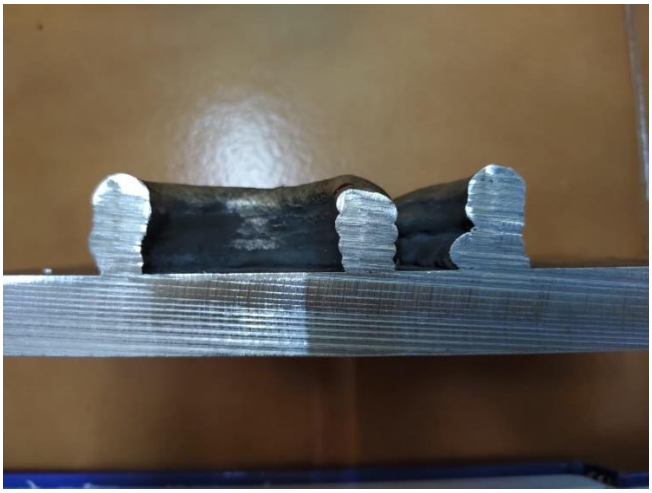

Fig 2.13 Cross-sectional view of the impeller

Facing and milling is performed to obtain acceptable surface finish. Fig 2.14 and Fig 2.16 pictures of impeller before final machining. Fig 2.15 and Fig 2.17 displays final product obtained through WAAM.

Fig 2.14 Before Machining top view

Fig 2.15 After Machining top View

Fig 2.16 Before Machining Side View

Fig 2.17After Machining Side view

Fig 2.18 Milling

Results and Discussion

Scanning Electron Microscope (SEM) Analysis

Performing an optical analysis on the workpiece surface using Scanning Electron Microscope (SEM) results in the identification of the interaction between metals, in our project interaction between two layers. A small piece cut from the printed part is observed under an Electron microscope at resolutions 50µm, 100µm, and 200µm.

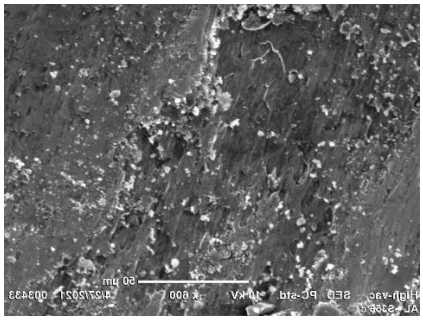

Fig 3.1 50µm

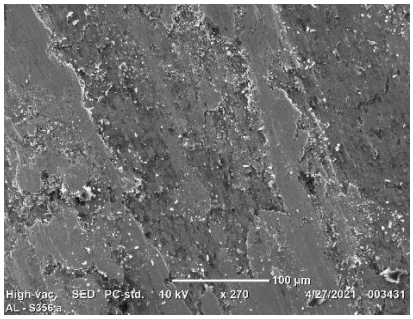

Fig 3.2 100µm

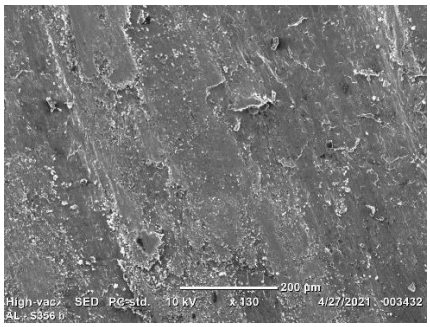

Fig 3.3 200µm

Corrosion Test (Salt Spray Test)

Salt Spray Test is a standardized test to obtain the corrosive resistance of the surface coating and materials. It is an accelerated corrosion test that conducts corrosive attacks on the sample to obtain results. The presence of corrosion or rust is calculated after a pre-determined time period. Time period is determined by the corrosion resistive properties of the material, high corrosion resistance materials have to undergo a long period of testing to obtain accurate results and low corrosion resistance materials have to undergo a relatively short period of testing to obtain final results. Table 3.1 comprises Test conditions for corrosion test.

Table 3.1 Corrosion Test Conditions

Total Duration (Hrs)	24
Chamber Temperature (^oC)	34.1 – 34.7
pH of solution	6.6
Air Pressure (psi)	15
Concentration of sodium Chloride (Percent)	5.2 – 5.5
Collection of Solution per Hour (ml)	1.2

Fig 3.4 Before Salt Spray **Fig 3.5 After Salt Spray**

No White or No Red Rust are Observed after 24 Hrs of Salt Spray Corrosion test

Wear Test

A wear test is performed to evaluate the wear property of a certain material under a certain wear condition to measure whether the material is acceptable for a specific wear condition.

Fig 3.6 Wear test specimen

Table 3.2 Wear Test Conditions

Cylinder Diameter (mm)	150
Cylinder Length (mm)	500
Material of corrosive abrasive sheet	60 Grade
Equivalent Rotation	84 times
Rotational Frequency (rpm)	40
Load Applied (Kg)	1

Table 3.3 Wear test Results

Initial Weight (g)	Final Weight (g)	Abrasion Loss	% loss
3.9187	3.8437	0.0750	1.91

Table 3.2 comprises of Wear test conditions. Table 3.3 comprises Wear test results. From the above wear test, we have obtained the result of 1.91% Weight loss due to wearing.

Chemical Composition Analysis

Chemical composition analysis is done on the impeller printed on 8mm and 16mm Aluminium (6061 Grade) plate. Table 3.4 consists of chemical composition of Al 4043 printed on 8mm plate and Table 3.5 consists of chemical composition of Al 4043 on 16mm plate.

Table 3.4 Chemical composition of Al 4043 on 8mm plate

Fe%	Si%	Mn%	Cu%	Ni%	Cr%	Ti%
0.157	4.552	<0.0.1	0.016	0.003	<0.005	0.018
Sn%	V%	Co%	Zn%	Pb%	Mg%	Al%
<0.006	0.006	<0.002	<0.02	0.005	<0.01	95.217

Table 3.5 Chemical composition of Al 4043 on 12mm plate

Fe%	Si%	Mn%	Cu%	Ni%	Cr%	Ti%
0.157	4.589	<0.0.1	0.015	0.004	<0.005	0.018
Sn%	V%	Co%	Zn%	Pb%	Mg%	Al%
<0.006	0.006	<0.002	<0.02	0.006	<0.01	99.18

Brinell Hardness Test

Brinell Hardness Test involves applying constant force for a definite time period using a tungsten carbide ball. Brinell Hardness test used to calculate surface hardness. Brinell Hardness test is conducted on both impellers printed on 8mm plate and 16mm plate. The test method conducted is ASME E10: 2018

Table 3.6 Brinell Hardness Test Results

Workpiece	Test	Result
8mm Plate	Hardness (10mm ball dia/500Kgf)	38.9, 38.1, 39.4
12mm Plate	Hardness (10mm ball dia/500Kgf)	40.2, 38.5, 40.4

3.1 Defects

While Wire Arc Additive Manufacturing (WAAM) boasts its advantages such as high deposition rates, low investments, But WAAM has some disadvantages regarding the manufactured/Printed part. Some of the defects are pores formation, rapid oxidation of some metals, and residual stress. Metals such as Titanium show very high oxidation while welding. Oxidation can be controlled by using a closed chamber filled with a combination of inert gasses. Porosity can be reduced by using correct shielding gas, gas flow rate and deposition strategy along with many more.

Bending due to residual stress is observed in both 8mm (Fig 3.8) and 16mm (Fig 3.7) plates. Porosity formation is also observed in the manufactured part. Fig 3.9 shows clear formation of the hole.

Fig 3.7 Deformation due to residual stress (16mm base plate)

Fig 3.8 Deformation due to residual stress (8mm base plate)

Fig 3.9 Porosity formation

Conclusion

A Detailed experimental and numerical study has been carried out to understand the process of Wire Arc Additive Manufacturing. The impeller is fabricated using Wire Arc Additive Manufacturing with pre-defined parameters (Voltage, Current, Feed speed etc). Conclusion for experimental hardness, corrosion test, and detailed experimental and theoretical study of SEM Analysis to better understand the fusion of layers.

- Optimization of process parameters for welding is done.
- Brinell Hardness Number of Al 4043 welded on 8mm plate is found to be 39.4
- Brinell Hardness Number of Al 4043 welded on 16mm plate is found to be 40.4
- Change in chemical composition is observed due to varying welding parameters.
- Increasing the thickness of the base plate reduces deformation due to residual stress.

Although WAAM produces near shape product, different materials produce different final finishes, some better than others. Al5356 produces more refined parts than Al4043.

References

1. A A Kulikov, A V Sidorova and A E Balanovskiy (2020) Process Design for the Wire Arc Additive Manufacturing of a Compressor Impeller
2. A. Queguineur, G. Rückert, F. Cortial, J. Y. Hascoët (2017) Evaluation of wire arc additive manufacturing for large-sized components in naval applications
3. Alexander Paolini, Stefan Kollmannsberger, and Ernst Rank (2019) Additive manufacturing in construction: A review on processes, applications, and digital planning methods
4. Ali Waqas1 , Qin Xiansheng1 , Xiong Jiangtao1 , Wang Hongbo1 , Muhammad Muzamil1 , Arfan Majeed1 (2019) Directional Tensile properties of steel structure manufactured by robotic assisted GMAW additive manufacturing
5. Bintao Wua, Zengxi Pana, Donghong Dingb, Dominic Cuiuria, Huijun Lia, Jing Xuc, John Norrish (2018) A review of the wire arc additive manufacturing of metals: properties, defects and quality improvement
6. Derekar, K. (2018) A review of wire arc additive manufacturing and advances in wire arc additive manufacturing of aluminum
7. Donghong Ding, Zengxi Pan, Dominic Cuiuri, Huijun Li (2015) Process planning for robotic wire and arc additive manufacturing.
8. Fernando Veiga, Alain Gil Del Val, Alfredo Suárez and Unai Alonso (2020) Analysis of the Machining Process of Titanium Ti6Al-4V Parts Manufactured by Wire Arc Additive Manufacturing (WAAM)
9. Filippo Montevecchia, Giuseppe Venturinia , Antonio Scippaa , Gianni Campatellia (2016) Finite element modelling of Wire-Arc-Additive-Manufacturing process
10. J. Lizarazu, L. Göbel1, S. Linne1, S. Kleemann, T. Lahmer, Ch. Rößler, J. Hildebrand (2020) Experimental characterization and numerical analysis of additively manufactured mild steel under monotonic loading conditions.
11. Lei Yuan, Donghong Ding, Zengxi Pan, Membe, Ziping Yu, Bintao Wu, Stephen van Duin, Huijun Li, Weihua Li (2019) Application of Multi-directional Robotic Wire Arc Additive Manufacturing Process for The Fabrication of Complex Metallic Parts
12. Xiangman Zhou, Haiou Zhang and Guilan Wang (2016) Three-Dimensional numerical simulation of arc and metal transport for Stacking deposition in Arc welding based Additive Manufacturing